Continuum Background Reduction in Orthogonal-Acceleration Time-of-Flight Mass Spectrometry with Continuous Ion Sources

Patrick P. Mahoney, Steven J. Ray, and Gary M. Hieftje
Department of Chemistry, Indiana University, Bloomington, Indiana, USA

Gangqiang Li
Hewlett Packard Laboratories, Palo Alto, California, USA

The continuum ion background in an inductively coupled plasma time-of-flight mass spectrometer (TOFMS) has been reduced by 2 orders of magnitude by using energy discrimination (ED). A potential barrier placed in front of the ion detector effectively discriminates between higher-energy signal ions and the lower-energy background ions. The signal-to-noise ratio was increased tenfold and detection limits of 0.4–4.2 ppt were achieved for 11 elements ranging from Li to U. The resolving power was observed to degrade from 1520 to 1230 with the addition of the potential barrier. The residual background count rate was found to be limited by neutrals formed after exiting the ion reflectron via charge exchange with the background gas. This ED method can be employed to effectively reduce the continuum ion background in any TOFMS that uses orthogonal acceleration with a continuous ion source. © *1997 American Society for Mass Spectrometry (J Am Soc Mass Spectrom 1997, 8, 125–131)*

Although the process of sampling ions from an atmospheric-pressure plasma into a mass spectrometer is an inefficient one [1], inductively coupled plasma mass spectrometry (ICPMS) has demonstrated excellent detection limits. The high signal-to-noise ratio (SNR) available in ICPMS is in large part attributable to the almost nonexistent background observed in ICPMS relative to that in inductively coupled plasma (ICP) emission spectrometry.

Quadrupole mass filters have almost exclusively been the mass analyzers of choice for ICPMS, owing to their high sensitivity, low operating costs, modest vacuum requirements, and the fact that they can accept ions of low energy. Low background levels were not observed with the first attempts at ICPMS; several configurations and techniques have been employed in quadrupole systems to reduce this background level below 10 counts per second (cps) with quadrupole mass analyzers [2]. A photon stop has been used effectively to block the intense photon and neutral flux emanating from the ICP. An offset ion detector can also be used to avoid false counts from these same species. More recently, various configurations of offset ion lenses have been used to reduce the photon and neutral background [3].

Address reprint requests to Dr. Gary M. Hieftje, Department of Chemistry, Indiana University, Bloomington, IN 47405.

Recently, a time-of-flight (TOF) mass analyzer has been shown to offer great potential for ICPMS [4–8]. By using a similar ion-sampling interface, the higher transmission efficiency of the time-of-flight mass spectrometer (TOFMS) should provide increased sensitivity over quadrupole mass analyzers. Also, unlike the scanned quadrupole mass analyzer, a TOFMS provides the full elemental and isotopic spectrum with each repeller event. This simultaneous detection capability not only shortens analysis times, but, coupled with the high repetition rate available with a TOFMS, also enables the analysis of transient signals with no compromise between sensitivity or precision and mass coverage.

The higher transmission efficiency of the TOFMS promises increased sensitivity, but the possibility of an elevated background also exists. Because the entrance to the flight tube is perpendicular to the path of the ions extracted from the ICP, photons and neutrals have no direct path to the ion detector; they are unaffected by the potentials used to extract the ions into the flight tube for mass separation. However, ions that enter the flight tube during time periods when the TOF extraction pulse is turned off, enabling the flight-time analysis, or those that follow a different path through the flight tube than desired, can appear as background upon which analyte peaks must be measured.

The primary source of ion background in this first-generation inductively coupled plasma time-of-

1044-0305/97/$17.00
PII S1044-0305(96)00199-7

Received June 21, 1996
Revised September 9, 1996
Accepted September 9, 1996

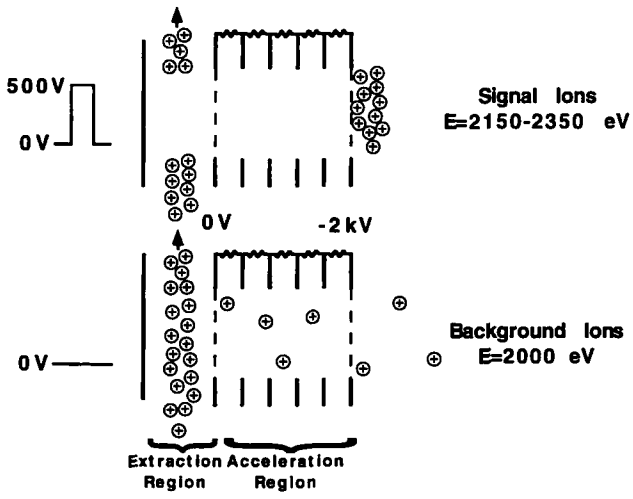

Figure 1. Schematic illustrating properly extracted signal ions (top) and "leakage" ions that contribute to the continuum background (bottom) in an orthogonal-acceleration TOFMS with continuous ion sources. The energies of the two types of ions are shown at the right. The signal ions receive a distribution of energies resulting from their original starting position along the potential gradient in the extraction region formed by the repeller pulse (left). While the repeller pulse is off, no gradient exists and the maximum energy of the "leakage" ions is 2000 eV.

flight mass spectrometer (ICP-TOFMS) [5] results from ion leakage as depicted in Figure 1. Shown in Figure 1 is a schematic of the extraction and acceleration regions of a typical Wiley–McLaren TOF spectrometer [9]. The ICP-generated ions enter the extraction region from the bottom and exit at the top. The top diagram shows the regions during a single repeller pulse. While the repeller (left-hand) plate is at an elevated potential, a linear potential gradient exists in the repeller region and an ion packet is pushed into the acceleration region, wherein they are accelerated by an additional 2 kV through the electrostatic field. Depending upon their initial starting position in the extraction region, the ions therefore exit the acceleration region and enter the flight tube with kinetic energies ranging from 2000 to 2500 eV. In Figure 1, the width of the ion beam is only ~ 40% of the extraction region width; thus the ions shown have energies ranging from approximately 2150 to 2350 eV. The bottom diagram in Figure 1 depicts these regions while the repeller plate is at low potential. Even when no potential gradient exists in the extraction region, the ions can still enter the acceleration region for at least two reasons: (1) Because the entrance to the acceleration region is a grid, the potential from the acceleration region can "leak" into the extraction region. Ions near the entrance grid can then be accelerated into the flight tube. (2) Even in the absence of leakage fields, ions that have appreciable perpendicular velocities can also enter the acceleration region. Although the supersonic expansion formed in the sampling interface minimizes this perpendicular velocity component, the ion optics, fringing fields, and scattering from surfaces can alter the trajectories of the ions. Space–charge repulsion or collisions with residual gas molecules can also change the ion velocity components. In either case, the ions are then accelerated to an energy of 2000 eV, enter the flight tube, and appear as a continuum background.

Because the ICP produces a continuous ion beam, the background caused by leakage ions appears as a continuum across the spectrum of interest. Given that these ions are accelerated to 2000 eV, and therefore have a slightly longer flight time for any given mass than the higher-energy signal ions, it is the ions that "leak" into the acceleration region during the microseconds before or after the extraction pulse that appear as ion background. For example, the flight time of 2000-eV Ar^+ (Ar is by far the most abundant species in the plasma and is likely the largest component of the ion background) along a 2-m flight path is approximately 20 μs; the flight times from $^1H^+$ to $^{238}U^+$ in the present instrument range from 3 to 55 μs. It is then the ions that "leak" into the acceleration region during the time period 17 μs prior to and 35 μs after the repeller pulse that become the problematic ion background. Given the 60-μs sampling period of the instrument (i.e., a 16.6-kHz repeller repetition frequency), almost all of the leakage ions contribute to the continuum background.

Several techniques have been used to reduce the ion background in the ICP-TOFMS [6]. To lessen the leakage fields from the acceleration region, a double grid can be installed. A double grid, however, does not deter ions with perpendicular velocity components unless the second grid is biased at a higher potential than the first. Also, a small positive or negative bias voltage (1–10 V) can be applied to the acceleration grid or to the repeller, respectively, to compensate for perpendicular velocities. However, increasing these voltages spoils the field-free conditions in the extraction region and can both degrade resolving power and compromise transmission efficiency. A more complicated but effective approach has been to modulate the ion beam so only the ions that would be successfully extracted into the flight tube were allowed into the extraction region [6]. This technique, called pulsed ion injection, employs a pulse applied to one of the quadrupole lenses prior to the extraction pulse to sweep the ion beam across a slit at the end of the ion-optic chain.

In the present study, a potential barrier has been placed in the flight path for energy discrimination (ED) between the higher-energy signal ions and the lower-energy background ions, as depicted in Figure 2. The barrier is constructed by placing three grids before the detector. The outer two grids are at flight-tube potential, while the potential of the center grid is adjustable to form a potential barrier between the first and second grids (see Figure 2). If the potential-barrier height is between the energies of the signal (bold) and background ions, only the signal ions are detected. The use of potential barriers for ED is well known in TOF mass

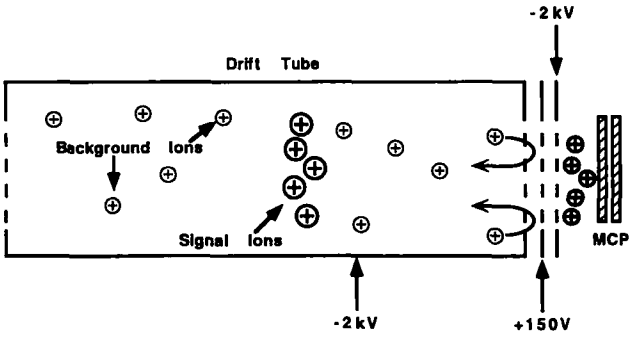

Figure 2. Pictorial representation of energy discrimination (ED). Lower-energy (2000-eV) background ions are repelled by the barrier formed by the three grids in front of the detector. Higher-energy (2150–2350-eV) signal ions pass through the barrier and are detected. MCP is a microchannel-plate detector.

spectrometry for the study of metastable fragmentation [10–12]. With an intense source, such as an ICP, ED is an efficient way to reduce the continuum-background level.

Experimental

Inductively Coupled Plasma Time-of-Flight Spectrometer

The ICP-TOFMS employed in these studies has been described previously [4–7]. Recent modifications to the three-stage interface and the ion optics that raised the ion current entering the extraction region and thus the sensitivity have also been presented [13]. The higher ion current, measured at the Faraday cup at the exit of the extraction region, also caused a dramatic increase in the continuum ion background over values reported previously [6]. A diagram of the current instrument is shown in Figure 3. Plasma conditions and typical ion-optic voltages are listed in Table 1. For this study, three grids were mounted 25 mm in front of the reflectron microchannel plate (MCP) detector [5]. The grids were constructed by spot welding wire mesh (28 lines/cm) onto 40-mm-i.d. stainless steel rings. The three rings were separated by 2-mm ceramic spacers.

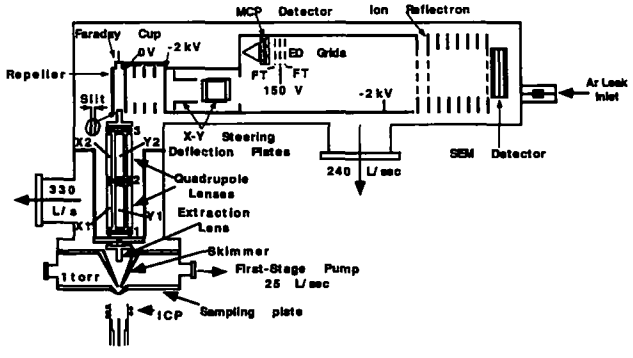

Figure 3. Diagram of the TOFMS instrument. ED grids are mounted 25 mm in front of detector 2 (reflectron detector). FT = flight-tube potential (−2 kV); MCP = microchannel-plate detector; SEM = secondary electron multiplier detector.

Table 1. Operating conditions

Plasma parameters	
ICP forward power	1.3 kW
ICP reflected power	< 5 W
Central-channel flow rate	1.2 L/min
Intermediate flow rate	1.0 L/min
Outer flow rate	13.5 L/min
Sampler-load coil distance	10 mm
TOFMS parameters	
Sampler aperture diameter	0.8 mm
Skimmer aperture diameter	0.9 mm
Third-stage aperture diameter	1.3 mm
Extraction lens voltage	−900 V
Lens 1 voltage	−600 V
Lens 2 voltage	−400 V
Lens 3 voltage	−200 V
Slit voltage	−150 V
X1	−30 V
Y1	+30 V
X2	+4 V
Y2	0 V
Repeller frequency	16.6 kHz
Repeller voltage pulse height	500 V
Acceleration voltage	−2000 V

The outer two grids were connected directly to flight-tube potential (−2 kV) to minimize their perturbation to the field-free region, whereas the center grid was connected to a power supply capable of providing 0–800 V (Keithley, Cleveland, OH, model 240A). For studies in which no potential barrier was desired, the center grid was held at the flight-tube potential. Unless otherwise specified, all experiments were conducted in the reflectron mode of operation [6]. A pair of 40-mm-diameter microchannel plates (Galileo Electro-Optics, Sturbridge, MA) in a chevron configuration was used as the detector. The front of the top plate was held at −5 kV to provide postacceleration and sufficient sensitivity for high-mass ions. In linear-mode operation, an electron multiplier detector (Hammamatsu, model R2363) was employed, which was biased at −2500 V.

For those studies in which the background level was measured as a function of flight-tube pressure, a controlled Ar leak was introduced into the third stage of the instrument. Pressure was controlled by two valves connected at the flange immediately behind the secondary electron multiplier detector and was monitored with a hot-cathode ion gauge (Varian Associates, Walnut Creek, CA).

Data Acquisition

Three methods of data acquisition were employed in these studies, all of which have been described previously [7, 8]. For the measurement of ion count rates and the calculation of detection limits, a single-channel ion-counting scheme was used. The amplified MCP

signal was directed to a constant-fraction discriminator (Tennelec, Oak Ridge, TN, model TC454), which was gated at the mass-to-charge ratio value of interest; the output pulses from the discriminator were sent to a digital counter (Hewlett-Packard, Palo Alto, CA, model 5334B). For high-speed two-channel analog detection, a pair of boxcar averagers (Stanford Research Systems, Stanford, CA, model SR250) was used. Full spectra were averaged and collected with a 500-MHz digital oscilloscope (Tektronix, Beaverton, OR, model TDS 520). The outputs of the counter, boxcar averagers, and the oscilloscope were recorded with a computer (Macintosh Quadra 950, Apple Computer, Cupertino, CA) and LabVIEW II software (National Instruments, Austin, TX).

All solutions were prepared through serial dilution of 1000 ppm standards (Johnson Mathey, Ward Hill, MA) of the appropriate species and introduced via a locally constructed ultrasonic nebulizer with desolvation.

Results and Discussion

To evaluate the extent to which the continuum ion background can be reduced with ED, the ion count rate was measured for various elements and their respective backgrounds as a function of the ED potential-barrier height. Figure 4 shows the result for rhodium. The signal count rate is that for the introduction of a 1-ng/mL solution and is measured with the single-channel ion-counting system described in the preceding text. The background was taken 1 mass unit away from the analyte peak (where no analyte peak was known to exist) so that only continuum background was measured. Off-peak values were needed due to impure blank solutions and/or a long washout time in the sample-introduction system. Plots similar to Figure 4 were obtained for all elements studied.

In Figure 4, the background count rate drops sharply from ~ 800 to ~ 8 cps as the barrier height exceeds 2100 V. No reduction in the signal count rate is observed for potential barrier heights below 2160 V. However, the signal did go down, as expected, at a higher barrier potential, owing to the finite energy obtained by the signal ions. Figure 4 is a stopping-potential curve and reveals the energy distributions of the signal and background ions. The sharp decrease in the background count rate above 2150 V suggests a narrow energy distribution. The signal-ion curve falls off more gradually, as expected, showing that the signal ions have a broader range of energies obtained from the potential gradient in the extraction region. The energy discrimination potentials required to reduce the signal and background count rates to half of the initial values were higher than was expected (2150 and 2450 V instead of 2000 and 2250 V for background and signal ions, respectively). This is likely attributable to the fact that the ED grids are so closely spaced that the effective potential is slightly lower than the applied potential, due to leakage fields. When the grids were separated by a greater distance, both the signal and background ions were stopped at the expected potentials. In the present study, the grids must be placed close together to minimize the perturbation to the field-free conditions in the flight tube and the effect on resolving power.

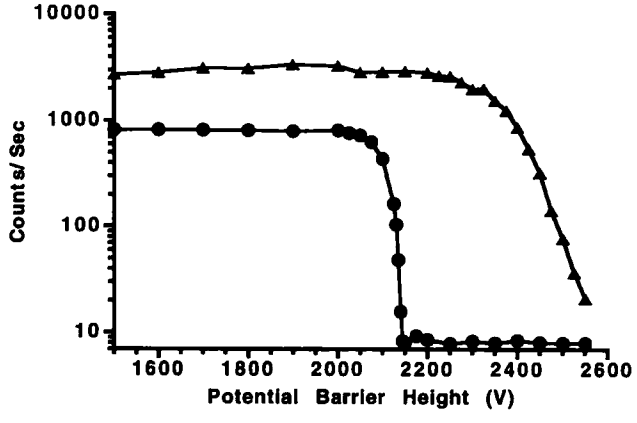

Figure 4. Signal (triangles) and adjacent background (circles) count rates as a function of potential-barrier height for 1-ppb ^{103}Rh solution.

Table 2 shows the improvement in detection limits (3σ) that ED provides for 11 elements across the elemental mass range. For the calculation of detection limits, the signal was defined as the average of five replicate 10-s integrations of the counts at the major isotope of the element of interest and the noise was taken as the standard deviation of 10 replicate 10-s integrations either at the mass-to-charge ratio value of interest (on-peak values) or at an adjacent mass-to-charge ratio value (off-peak values). Due to blank impurities and/or a long washout time of the sample-introduction system, off-peak values better demonstrate the continuum-background reduction. Impurities and memory effects would result in a higher energy (2150–2350-eV) background. The off-peak values were obtained by measuring the background 1–2 mass units away from the analyte peaks to simulate the detection limits that would be available under clean-room conditions. The detection limits were measured with and without a potential barrier of 2160 V present in front of the detector. For each element, a 10fold reduction in detection limits is observed, as would be predicted by counting statistics for a 100fold reduction in background count rates.

Table 2 also illustrates a trend that the detection limits are higher (worse) for the lighter elements, especially Mg. The signal count rates are similar to those for the heavier elements; however, the detection limits are compromised by a slightly elevated background for these lighter elements. This background is likely due to scattered high-energy (> 2000-eV) ions that are attributable to at least two sources. First, to avoid saturation of the MCP, the dense $^{40}Ar^+$ ion packets are deflected out of the flight path with a positive pulse

Table 2. Limits of detection with (W) and without (W/O) energy discrimination (ED)

Element	Detection limit[a] (ng/L)		
	Off peak w/o ED	Off peak w/ED	On peak w/ED
Li	11.6	1.5	1.9
Mg	34.3	4.2	7.5
Mn	15.1	1.5	6.8
Co	8.4	1.1	2.0
Sr	4.3	0.6	2.2
Rh	6.3	0.5	1.5
Ag	9.8	0.9	2.6
Cs	5.4	0.5	3.0
Ho	4.5	0.4	1.7
Bi	7.8	0.6	5.2
U	7.6	0.6	5.6

[a] Off peak indicates that background-noise readings were taken in a signal-free region adjacent to the mass-spectral peak of interest. On peak signifies that background noise was measured at the mass-spectral peak of interest during aspiration of a blank solution. Energy barrier = 2160 V.

applied to one of the TOFMS steering plates. The deflected ions obtain a wide distribution of trajectories and can lead to increased background in unpredictable locations of the mass spectrum. These ions could perhaps be blocked with properly placed baffles in the flight tube to better define the path of the signal ions. Unfortunately, the ion beam is quite divergent in the present instrument [5], and this modification would likely lead to reduced transmission and sensitivity. Ions scattered from the optics and grids (acceleration and reflectron) might also contribute to the elevated background. If, indeed, such scattering is a major source of background, it would be expected to be most prominent in the vicinity of the peaks corresponding to the most abundant species. The most abundant species from the plasma are H^+, N^+, O^+, OH^+, H_2O^+, Ar^+, and Ar_2^+ at m/z 1, 14, 16, 17, 18, 40, and 80, respectively. Indeed, the background rises from ~ 10 to ~ 50 cps within 1 mass unit of these abundant species. This elevated background not only compromises detection limits, but imposes a limit on abundance sensitivity as well. An abundance sensitivity of greater than 10^5 has been reported for the present instrument [8].

Unfortunately, placing a potential barrier in the flight path has an adverse affect on resolving power. The energy-discrimination device, made of three grids before the ion detector, necessarily disturbs the energy-focusing condition of the ion reflector. Figure 5 shows three spectra, each of which arises from the average of 1000 repeller cycles. The first (Figure 5a) demonstrates the resolving power in the absence of a potential barrier. The resolving power (measured at half maximum) is 1520. With a potential barrier of 2160 V (Figure 5b), the flight times of the ions are increased by about 100 ns and the resolving power is reduced to 1060. With modest adjustment of the reflectron potentials (Figure 5c), the time error caused by the energy-discrimination grids can be partly compensated and a

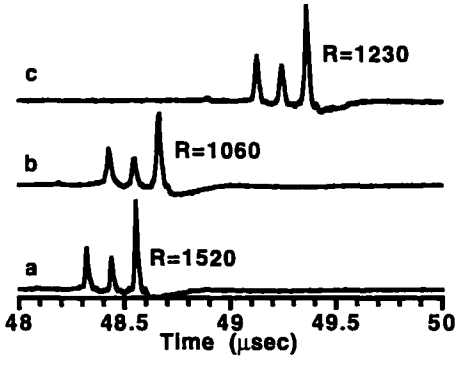

Figure 5. Effect of ED on resolving power. Each spectrum arises from the average of 1000 repeller cycles during nebulization of a 100-ppb Pb solution. Resolving power is measured at full width at half maximum for (a) no potential barrier, (b) barrier of 2160 V, and (c) barrier of 2160 V and minor adjustments to reflectron and ion-optic voltages.

resolving power of 1230 is recovered. A two-stage reflectron with a homogenous field distribution was utilized for this compensation, but the inhomogenous fields offered by a gridless reflectron could provide better energy focusing with the potential barrier in place. Nevertheless, the present resolving power is more than adequate to perform elemental analysis.

Another consequence of the potential barrier is that, even though grids were used, the large potential gradient acts like an ion lens. In principle, the barrier could be placed anywhere in the flight path to discriminate against the background ions. Three different locations were evaluated in this study. A potential barrier of 10–30 V placed immediately after the extraction region reduced the ion noise to the same extent as described in the foregoing text, as did a 2050-V barrier placed immediately after the acceleration region. However, the lens effect of the barrier reduced the transmission efficiency considerably in both cases. For this reason,

the reported results are those obtained when the barrier was placed 25 mm in front of the MCP detector.

Although the use of ED dramatically lowers the continuum background, inspection of the background curve in Figure 4 reveals that a finite count rate exists even when the barrier height exceeds 2500 V. These counts are not due to dark events from the detector; with the ion optics turned off and/or the plasma extinguished, the count rate is less than 0.1 cps for the MCP detector. Because the signal ions possess an energy greater than the potential-barrier height, it is not surprising that some background ions could have energies greater than 2000 but less than 2500 eV. Surprisingly, as the potential barrier is raised above 2800 V (note that the maximum possible energy of any ion is 2500 eV), the background counts remain. In fact, with high amplification, an entire spectrum of the most abundant species (H^+, N^+, O^+, and Ar^+) was observed even in the presence of a 2800-V barrier height. Because source-generated ions could not have such high energy, two explanations are plausible. One is that the ions do not go through the ED grids but somehow reach the detector along another path. The fact that these peaks occur at the same flight times as the abundant species when the barrier is at 0 V argues against this hypothesis. Furthermore, when the ED grids were replaced with a solid plate, only dark counts were observed.

Alternatively, the peaks might result from species that do not experience the electric field (i.e., neutrals). Ferguson et al. [10] described a similar instrumental arrangement utilized to study secondary processes that occur after acceleration in the TOFMS. In their studies, a retarding field was used to discriminate against ions and to facilitate the study of neutral species. To verify the presence or absence of neutrals as a source of continuum background in the present experiment, the instrument was used in the linear mode of operation [6] and the ion reflectron was operated as an energy-discrimination device. In this case, ions (and neutrals) were detected by the electron multiplier detector located behind the reflectron. Figure 6 shows the effect of increasing the potential-barrier height on the O^+ peak shape. Omitted from Figure 6 is the single peak that is observed at the 0-V barrier (i.e., the reflectron grids are held at flight-tube potential), but above a barrier height of 2200 V a small peak becomes evident as the larger peak, due to O^+, is displaced to longer flight times. This small peak is presumably from neutral O, as its flight time does not increase with barrier height. The O^+ signal, however, is delayed, broadened, and attenuated considerably as the barrier height rises to match the energies of the signal ions. The attenuation of the O^+ peak is in accordance with the expected energies of the signal ions. Furthermore, the considerable distance over which the discrimination occurs (about 50fold wider than the barrier in front of the reflectron detector) in the reflectron serves as an extreme example of the degradation of resolving power

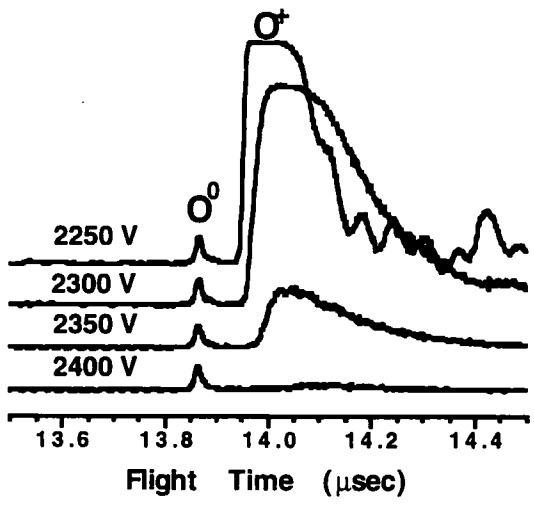

Figure 6. Portion of spectrum showing peaks corresponding to oxygen ions and oxygen neutrals. The neutrals (formed from ions with trajectories toward the detector) are unaffected by the potential barrier. The ion signal is delayed, broadened, and attenuated as the barrier height matches and exceeds the energies of the signal ions.

that occurs when the barrier height is increased. The peak broadens because the large and wide potential barrier spoils the space-focusing conditions.

Although the ICP serves as a strong source of neutral Ar, the species that enter the spectrometer as neutrals from the ICP are not likely to reach the detector in this right-angle geometry. Neutrals are unaffected by the potentials used to extract the ions into the perpendicular flight tube, steer the ions, and turn the ions around (reflectron) to reach the detector. To reach the reflectron detector, neutrals must be formed from the ions that have already exited the reflectron and have the proper trajectory toward the detector. These neutrals must then be formed via charge exchange with either grid surfaces or residual gas molecules. The former possibility was explored by removing the reflectron grids and the front ED grid. Upon removal of the reflectron grids, the ion transmission was increased by 20% and the resolving power remained the same, as did the neutral peak heights. Removal of the first ED grid degraded the resolving power drastically, as leakage fields extended into the flight tube. The neutral intensity remained the same and the first ED grid was subsequently replaced.

To test if charge exchange with residual gas molecules was the mechanism of neutral-species formation, the background gas pressure was raised by allowing Ar to enter the third stage through two valves in series (see Figure 3). Figure 7a shows the dependence of the Ar and O neutral peak areas on flight-tube pressure from 2 to 7 μtorr for a potential barrier of 2550 V. Each point on the plot represents a software integration of the peak areas in the neutrals spectrum obtained with the digital oscilloscope (average of 500 spectra). Figure 7b shows the continuum background

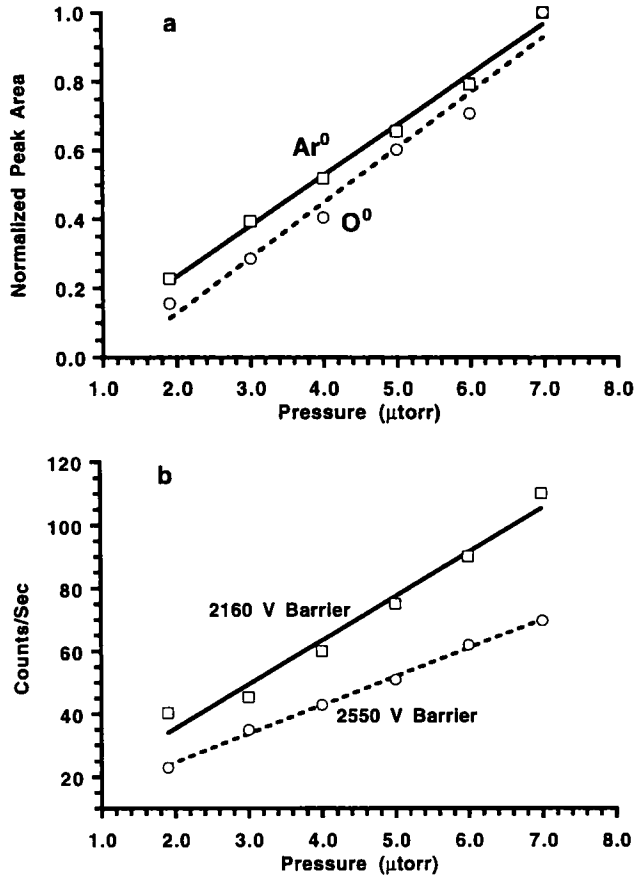

Figure 7. (a) Magnitude of neutral peaks observed at a potential-barrier height of 2800 V as a function of flight-tube pressure. The maximum possible ion energy is 2500 eV. Linear dependence suggests that charge exchange with the background gas is the cause of the neutral species formed from ions exiting the reflectron with trajectories toward the detector. (b) Continuum background count rate as a function of flight-tube pressure for a potential barrier height of 2160 V (squares) and 2550 V (circles). Linear dependence suggests that charge exchange with the background gas is the cause of the limiting background counts. The higher count rate for the 2160-V potential barrier height demonstrates that some of the background counts are due to higher-energy (> 2160-eV) ions.

count rate just before the Ar_2^+ peak (flight time of approximately 30 μs) as a function of pressure with a potential barrier of both 2160 and 2550 V. The linear dependence on pressure in all the plots of Figure 7 suggests that charge exchange with the background gas is the source of the neutral formation. Comparison of the count rates at the two barrier heights in Figure 7b shows that some of the background counts are due to high-energy ions (i.e., > 2000 eV). The presence of these high-energy ions is a result of scattering of the dense Ar_2^+ ion packet. These ions are discriminated against as the barrier is raised to 2550 V.

Conclusions

The utility of energy discrimination for the reduction of continuum background in an orthogonal-acceleration TOFMS with a continuous ion source was successfully demonstrated. The background level, which is now limited by counts from neutrals formed via charge exchange with the background gas, could be reduced further through a reduction in the third-stage pressure or an improvement in the focusing characteristics of the pre-extraction-region ion optics. An improvement in the focusing characteristics would reduce the number of leakage ions available for charge exchange with the residual gas molecules. Mass resolution is degraded somewhat when ED is utilized. However, the time error caused by the ED device might be compensated with an inhomogenous ion-reflectron field.

Acknowledgments

The authors wish to thank the National Institutes of Health (Grant R01 GM 53560) for financial support. One of the authors (PPM) thanks the Society for Analytical Chemists at Pittsburgh and Proctor and Gamble for fellowship support.

References

1. Douglas, D. J.; French, J. B. *J. Anal. At. Spectrom.* **1988,** *3,* 743–47.
2. Jarvis, K. E.; Gray, A. L.; Houk, R. S. *Handbook of Inductively Coupled Plasma Mass Spectrometry;* Chapman and Hall: New York, 1992.
3. Hu, K.; Clemons, P. S.; Houk, R. S. *J. Am. Soc. Mass Spectrom.* **1993,** *4,* 16–27.
4. Myers, D. P.; Hieftje, G. M. *Microchem. J.* **1993,** *48,* 259–277.
5. Myers, D. P.; Li, G.; Yang, P.; Hieftje, G. M. *J. Am. Soc. Mass Spectrom.* **1994,** *5,* 1008–1016.
6. Myers, D. P.; Li, G.; Mahoney, P. P.; Hieftje, G. M. *J. Am. Soc. Mass Spectrom.* **1995,** *6,* 400–410.
7. Myers, D. P.; Li, G.; Mahoney, P. P.; Hieftje, G. M. *J. Am. Soc. Mass Spectrom.* **1995,** *6,* 411–420.
8. Myers, D. P.; Mahoney, P. P.; Li, G.; Hieftje, G. M. *J. Am. Soc. Mass Spectrom.* **1995,** *6,* 920–927.
9. Wiley, W. C.; McLaren, I. H. *Rev. Sci. Instrum.* **1955,** *26,* 1150–1157.
10. Ferguson, R. E.; McCulloh, K. E.; Rosenstock, H. M. *J. Chem. Phys.* **1965,** *42,* 100–106.
11. Ryan, P. W.; Futrell, J. H.; Vestal, M. L. *Chem. Phys. Lett.* **1973,** *18,* 329–332.
12. Chait, B. T.; Field, F. H. *Int. J. Mass Spectrom. Ion Phys.* **1981,** *41,* 17–29.
13. Mahoney, P. P.; Li, G.; Hieftje, G. M. *J. Anal. At. Spectrom.* **1996,** *11,* 401–405.